

Skin values and matter radii of ^{208}Pb and $^{58,60,64}\text{Ni}$ based on reaction cross section of $^{3,4}\text{He}$ scattering

Shingo Tagami, Tomotsugu Wakasa, and Masanobu Yahiro

Background: The PREX group reported a new skin value, $r_{\text{skin}}^{208}(\text{PREX2}) = 0.283 \pm 0.071 = 0.212 \sim 0.354$ fm. Using the chiral (Kyushu) g -matrix folding model with the proton and neutron densities determined with D1S+GHFB+AMP, we determined neutron skin thickness $r_{\text{skin}}^{208}(\text{exp}) = 0.278 \pm 0.035$ fm from reaction cross sections $\sigma_{\text{R}}(\text{exp})$ of $\text{p}+^{208}\text{Pb}$ scattering, where D1S-GHFB+AMP denotes Gogny-D1S HFB with angular momentum projection (AMP). The method also yielded $r_{\text{skin}}^{208}(\text{exp}) = 0.416 \pm 0.146$ fm from $\sigma_{\text{R}}(\text{exp})$ of $^4\text{He}+^{208}\text{Pb}$ scattering. In our previous work, we accumulated the 206 EoSs and determined a slope parameter $L = 76 \sim 165$ MeV from the 206 EoSs. The value of L yields $r_{\text{skin}}^{208} = 0.102 \sim 0.354$ fm. As for ^{58}Ni , a novel method for measuring nuclear reactions in inverse kinematics with stored ion beams was successfully used to extract matter radii r_{m} of ^{58}Ni at the GSI facility.

Purpose: As the first aim, we first determine $r_{\text{skin}}^{208}(\text{exp})$ from $\sigma_{\text{R}}(\text{exp})$ of ^3He scattering on ^{208}Pb target and take the weighted mean and its error for $r_{\text{skin}}^{208}(\text{PREX2})$, three skin values of $\text{p}+^{208}\text{Pb}$, $^3\text{He}+^{208}\text{Pb}$ scattering and $r_{\text{skin}}^{208} = 0.102 \sim 0.354$ fm based on the 206 EoSs. As the second aim, we determine matter radii $r_{\text{m}}(\text{exp})$ of $^{58,60,64}\text{Ni}$ from $\sigma_{\text{R}}(\text{exp})$ of $^{3,4}\text{He}$ scattering on $^{58,60,64}\text{Ni}$ targets.

Results: Our result is $r_{\text{skin}}^{208}(\text{exp}) = 0.512 \pm 0.268$ fm for $^3\text{He}+^{208}\text{Pb}$ scattering. Our results based on $^4\text{He}+^{58,60,64}\text{Ni}$ scattering are $r_{\text{m}}^{58}(\text{exp}) = 3.734 \pm 0.091$ fm, $r_{\text{m}}^{60}(\text{exp}) = 3.815 \pm 0.094$ fm, $r_{\text{m}}^{64}(\text{exp}) = 4.001 \pm 0.093$ fm. Our results based on $^3\text{He}+^{58,60,64}\text{Ni}$ scattering are $r_{\text{m}}^{58}(\text{exp}) = 3.709 \pm 0.098$ fm, $r_{\text{m}}^{60}(\text{exp}) = 3.753 \pm 0.112$ fm, $r_{\text{m}}^{64}(\text{exp}) = 3.822 \pm 0.142$ fm.

Conclusion: Our conclusion is $r_{\text{skin}}^{208} = 0.285 \pm 0.030$ fm. It is determined from the 5 skin values mentioned above.

I. INTRODUCTION AND CONCLUSION

Background:

Horowitz, Pollock and Souder proposed a direct measurement for neutron skin thickness $r_{\text{skin}} = r_{\text{n}} - r_{\text{p}}$ [1], where r_{p} and r_{n} are proton and neutron radii, respectively. This direct measurement consists of parity-violating and elastic electron scattering. In fact, the PREX collaboration has reported,

$$r_{\text{skin}}^{208}(\text{PREX2}) = 0.283 \pm 0.071 = 0.212 \sim 0.354 \text{ fm}, \quad (1)$$

combining the original Lead Radius EXperiment (PREX) result [2, 3] with the updated PREX2 result [4]. This measurement is a direct one yielding a neutron skin thickness r_{skin}^{208} . The $r_{\text{skin}}^{208}(\text{PREX2})$ is determined with weak electromagnetic interaction.

Many theoretical predictions on the symmetry energy $S_{\text{sym}}(\rho)$ have been made so far. In neutron star, the $S_{\text{sym}}(\rho)$ and its density (ρ) dependence influence strongly the nature within the star. The symmetry energy $S_{\text{sym}}(\rho)$ cannot be measured by experiment directly. In place of $S_{\text{sym}}(\rho)$, the neutron-skin thickness r_{skin} is measured to determine the slope parameter L , since a strong correlation between r_{skin}^{208} and L is well known [5]. In fact, the relation of Ref. [5] yields $L = 76 \sim 172$ MeV from $r_{\text{skin}}^{208}(\text{PREX2})$. As shown later in Eq. (3), we also determine the relation yielding $L = 76 \sim 165$ MeV.

Meanwhile, reaction cross section σ_{R} is a standard observable for determining matter radius r_{m} and skin value r_{skin} . High-accuracy data $\sigma_{\text{R}}(\text{exp})$ with 2% error are available for $\text{p} + ^{208}\text{Pb}$ scattering in $21 \leq E_{\text{lab}} \leq 100$ MeV [6–8]. The chiral (Kyushu) g -matrix folding model with the D1S-GHFB+AMP yields $r_{\text{skin}}^{208}(\text{exp}) = 0.278 \pm 0.035$ fm [9], where D1S-GHFB+AMP stands for Gogny-D1S HFB with angular momentum projection (AMP). The value is consistent with $r_{\text{skin}}^{208}(\text{PREX2})$. Data $\sigma_{\text{R}}(\text{exp})$ with 5% error are

available for $^4\text{He}+^{208}\text{Pb}$ scattering [10]. We then determined $r_{\text{skin}}^{208}(\text{exp}) = 0.416 \pm 0.146$ fm in $29 \leq E_{\text{lab}} \leq 48$ MeV per nucleon [11]. In this paper, we firstly extract $r_{\text{skin}}^{208}(\text{exp})$ from $^3\text{He}+^{208}\text{Pb}$ scattering by using the Kyushu g -matrix folding model with the D1S-GHFB+AMP, although the data [10] on the σ_{R} have large 8.1% error.

As for ^{58}Ni , a novel method for measuring nuclear reactions in inverse kinematics with stored ion beams was successfully used to extract the r_{m} of ^{58}Ni [12]. The experiment was performed at the experimental heavy-ion storage ring at the GSI facility. Their result determined from the differential cross section for $^{58}\text{Ni}+^4\text{He}$ scattering is $r_{\text{m}}(\text{GSI}) = 3.70(7)$ fm for ^{58}Ni .

Data σ_{R} with 4 ~ 7% error are available for $^{3,4}\text{He}+^{58,60,64}\text{Ni}$ scattering [10].

A theoretical constraint on r_{skin}^{208} :

In Ref. [13], we accumulated the 206 EoSs from Refs. [5, 14–38] in which r_{skin}^{208} and/or L is presented, since a strong correlation between r_{skin}^{208} and a slope parameter L is shown. The 206 EoSs are shown in Table I of Ref. [13]. The correlation between L and r_{skin}^{208} is more reliable when the number of EoSs is larger. For this reason, we take the 206 EoSs. Using the 206 EoSs of Table I, we found the L - r_{skin}^{208} relation as

$$L(r_{\text{skin}}^{208}) = 620.39 r_{\text{skin}}^{208} - 57.963 \quad (2)$$

with a very high correlation coefficient $R = 0.99$ [13]; see Fig. 1. Note that a very high correlation coefficient means that Eq. (2) is concrete.

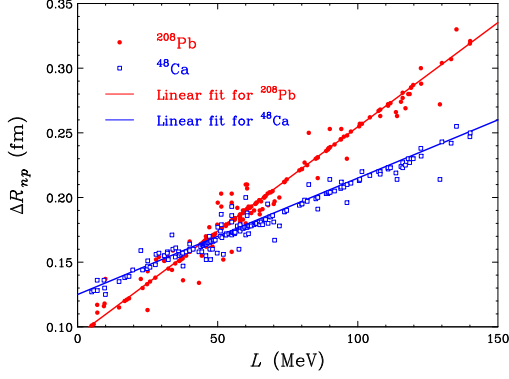


FIG. 1. Skin values $\Delta R_{np} \equiv r_{\text{skin}}$ as a function of L for ^{208}Pb and ^{48}Ca . The straight line shows Eq. (2) for ^{208}Pb and another line is $r_{\text{skin}}^{48} = 0.0009L + 0.125$ for ^{48}Ca . Dots denote 206 EoSs for ^{208}Pb and ^{48}Ca .

The 206 EoSs yields a theoretical constraint on L , i.e., $L = 5.020 \sim 161.05$ MeV. Using Eq. (2) and $L = 5.020 \sim 161.05$ MeV, we can derive a range of r_{skin}^{208} theoretically. The result is

$$r_{\text{skin}}^{208} = 0.102 \sim 0.354 \text{ fm.} \quad (3)$$

This is a theoretical constraint on r_{skin}^{208} . The upper bound of the theoretical constraint agrees with that of r_{skin}^{208} (PREX2). The r_{skin}^{208} (PREX2) supports stiffer EoSs.

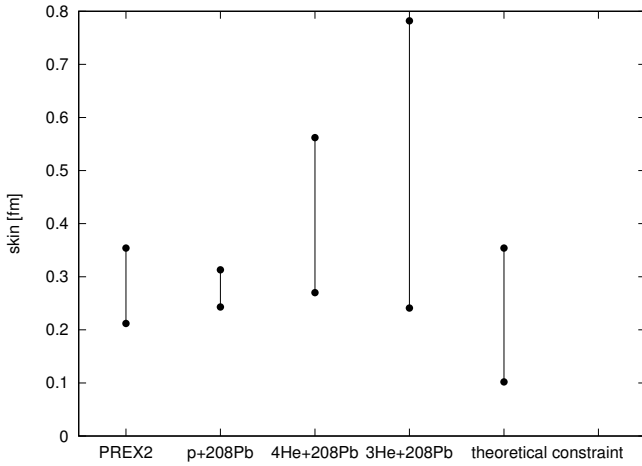


FIG. 2. r_{skin}^{208} (PREX2), three skin values determined from reaction cross sections σ_R of p , ^4He , ^3He scattering on ^{208}Pb target, the theoretical constraint of Eq. (3).

As for r_{skin}^{208} , therefore, we can summarize five skin-values; 1) PREX2, 2) p scattering, 3) ^4He scattering, 4) ^3He scattering, 5) the theoretical constraint of Eq. (3) in Fig. 2. The

skin value $r_{\text{skin}}^{208}(\text{exp})$ of $^3\text{He}+^{208}\text{Pb}$ scattering supports stiffer EoSs.

Aims:

As the first aim, we determine $r_{\text{skin}}^{208}(\text{exp})$ from the $\sigma_R(\text{exp})$ of $^3\text{He}+^{208}\text{Pb}$ scattering and take the weighted mean and its error for five skin values 1), 2), 3), 4), 5) shown in Fig. 2. As the second aim, we determine $r_m(\text{exp})$ of $^{58,60,64}\text{Ni}$ from the $\sigma_R(\text{exp})$ of $^3,^4\text{He}$ scattering on $^{58,60,64}\text{Ni}$ targets.

Results:

We first determine $r_{\text{skin}}^{208}(\text{exp})$ from $\sigma_R(\text{exp})$ [10] of $^3\text{He}+^{208}\text{Pb}$ scattering in $32 \leq E_{\text{lab}} \leq 56$ MeV per nucleon; the result is

$$r_{\text{skin}}^{208}(\text{exp}) = 0.512 \pm 0.268 = 0.243 \pm 0.780 \text{ fm,} \quad (4)$$

where E_{lab} is an incident energy per nucleon. The result is consistent with r_{skin}^{208} (PREX2) = $0.212 \sim 0.354$ fm.

We next evaluate $r_m^{58,60,64}(\text{exp})$ from $^3,^4\text{He}+^{58,60,64}\text{Ni}$ scattering. Our results for ^4He scattering are $r_m^{58}(\text{exp}) = 3.734 \pm 0.091$ fm, $r_m^{60}(\text{exp}) = 3.815 \pm 0.094$ fm, $r_m^{64}(\text{exp}) = 4.001 \pm 0.093$ fm, where the data taken is Ref. [10] for $^{58,60}\text{Ni}$ and is Ref. [39] for ^{64}Ni . Our results for ^3He scattering are $r_m^{58}(\text{exp}) = 3.709 \pm 0.098$ fm, $r_m^{60}(\text{exp}) = 3.753 \pm 0.112$ fm, $r_m^{64}(\text{exp}) = 3.822 \pm 0.142$ fm, where the data taken is Ref. [10] for $^{58,60,64}\text{Ni}$. Our results based on $^4\text{He}+^{58,60,64}\text{Ni}$ are consistent with those based on $^3\text{He}+^{58,60,64}\text{Ni}$. In addition, these results for ^{58}Ni are consistent with the r_m of Ref. [12].

Conclusion: We take the weighted mean and its error for five skin values 1), 2), 3), 4), 5) shown in Fig. 2. The skin value is

$$r_{\text{skin}}^{208} = 0.285 \pm 0.030 \text{ fm.} \quad (5)$$

This value is mainly determined by the skin value of $p+^{208}\text{Pb}$ scattering.

II. MEHOD

Our method is composed of the chiral (Kyushu) g -matrix folding model for scattering [40] and D1S-GHFB+AMP [41] for target densities, where D1S-GHFB+AMP stands for Gogny-D1S HFB with the angular momentum projection (AMP).

As for the symmetric nuclear matter, Kohno calculated the g matrix by using the Brueckner-Hartree-Fock (BHF) method with chiral N^3LO 2NFs and NNLO 3NFs [42]. The framework is applied for positive energies. The resulting non-local chiral g matrix is localized into three-range Gaussian forms by using the localization method proposed by the Melbourne group [43, 44]. The resulting local g matrix is referred to as Kyushu g -matrix in this paper [40].

The Kyushu g -matrix folding model was tested for ^{12}C scattering on ^9Be , ^{12}C , ^{27}Al targets in $30 \leq E_{\text{lab}} \leq 400$ MeV. We found that the Kyushu g -matrix folding model is good in $30 \leq E_{\text{lab}} \leq 100$ MeV and $250 \leq E_{\text{lab}} \leq 400$ MeV.

The brief formulation of the folding model itself is shown below. The potential U consists of the direct part (U^{DR}) and

the exchange part (U^{EX}):

$$U^{\text{DR}}(\mathbf{R}) = \sum_{\mu,\nu} \int \rho_{\text{P}}^{\mu}(\mathbf{r}_{\text{P}}) \rho_{\text{T}}^{\nu}(\mathbf{r}_{\text{T}}) g_{\mu\nu}^{\text{DR}}(s; \rho_{\mu\nu}) d\mathbf{r}_{\text{P}} d\mathbf{r}_{\text{T}}, \quad (6)$$

$$U^{\text{EX}}(\mathbf{R}) = \sum_{\mu,\nu} \int \rho_{\text{P}}^{\mu}(\mathbf{r}_{\text{P}}, \mathbf{r}_{\text{P}} - \mathbf{s}) \rho_{\text{T}}^{\nu}(\mathbf{r}_{\text{T}}, \mathbf{r}_{\text{T}} + \mathbf{s}) \times g_{\mu\nu}^{\text{EX}}(s; \rho_{\mu\nu}) \exp[-i\mathbf{K}(\mathbf{R}) \cdot \mathbf{s}/M] d\mathbf{r}_{\text{P}} d\mathbf{r}_{\text{T}}, \quad (7)$$

where $\mathbf{s} = \mathbf{r}_{\text{P}} - \mathbf{r}_{\text{T}} + \mathbf{R}$ for the coordinate \mathbf{R} between P and T. The coordinate \mathbf{r}_{P} (\mathbf{r}_{T}) denotes the location for the interacting nucleon measured from the center-of-mass of the projectile (target). Each of μ and ν stands for the z -component of isospin; $1/2$ means neutron and $-1/2$ does proton. The original form of U^{EX} is a non-local function of \mathbf{R} , but it has been localized in Eq. (7) with the local semiclassical approximation [45–47] in which P is assumed to propagate as a plane wave with the local momentum $\hbar\mathbf{K}(\mathbf{R})$ within a short range of the nucleon-nucleon interaction, where $M = AA_{\text{T}}/(A + A_{\text{T}})$ for the mass number A (A_{T}) of P (T). The validity of this localization is shown in Ref. [48].

The direct and exchange parts, $g_{\mu\nu}^{\text{DR}}$ and $g_{\mu\nu}^{\text{EX}}$, of the effective nucleon-nucleon interaction (g -matrix) are assumed to depend on the local density

$$\rho_{\mu\nu} = \sigma^{\mu} \rho_{\text{T}}^{\nu}(\mathbf{r}_{\text{T}} + \mathbf{s}/2) \quad (8)$$

at the midpoint of the interacting nucleon pair, where σ^{μ} is the Pauli matrix of a nucleon in P. This choice of the local density is quite successful for ${}^4\text{He}$ scattering, as shown in Ref. [49].

The direct and exchange parts are described by

$$\begin{aligned} & g_{\mu\nu}^{\text{DR}}(s; \rho_{\mu\nu}) \\ &= \begin{cases} \frac{1}{4} \sum_S \hat{S}^2 g_{\mu\nu}^{S1}(s; \rho_{\mu\nu}) & ; \text{ for } \mu + \nu = \pm 1 \\ \frac{1}{8} \sum_{S,T} \hat{S}^2 g_{\mu\nu}^{ST}(s; \rho_{\mu\nu}), & ; \text{ for } \mu + \nu = 0 \end{cases} \quad (9) \\ & g_{\mu\nu}^{\text{EX}}(s; \rho_{\mu\nu}) \\ &= \begin{cases} \frac{1}{4} \sum_S (-1)^{S+1} \hat{S}^2 g_{\mu\nu}^{S1}(s; \rho_{\mu\nu}) & ; \text{ for } \mu + \nu = \pm 1 \\ \frac{1}{8} \sum_{S,T} (-1)^{S+T} \hat{S}^2 g_{\mu\nu}^{ST}(s; \rho_{\mu\nu}) & ; \text{ for } \mu + \nu = 0 \end{cases} \quad (10) \end{aligned}$$

where $\hat{S} = \sqrt{2S+1}$ and $g_{\mu\nu}^{ST}$ are the spin-isospin components of the g -matrix interaction.

The proton and neutron densities, $\rho_{\text{p}}(r)$ and $\rho_{\text{n}}(r)$, are calculated with D1S-GHFB+AMP [41]. As a way of taking the center-of-mass correction to the D1S-GHFB+AMP densities, we use the method of Ref. [50], since the procedure is quite simple. For ${}^3, {}^4\text{He}$, we take the phenomenological densities of Ref. [51].

In order to deduce the r_{m} from $\sigma_{\text{R}}(\text{exp})$ [10, 52], we have to scale the proton and neutron densities, as shown in Sec. III. Now we explain the scaling of density $\rho(\mathbf{r})$. We can obtain

the scaled density $\rho_{\text{scaling}}(\mathbf{r})$ from the original density $\rho(\mathbf{r})$ as

$$\rho_{\text{scaling}}(\mathbf{r}) = \frac{1}{\alpha^3} \rho(\mathbf{r}/\alpha) \quad (11)$$

with a scaling factor

$$\alpha = \sqrt{\frac{\langle r^2 \rangle_{\text{scaling}}}{\langle r^2 \rangle}}. \quad (12)$$

As for ${}^{208}\text{Pb}$, $\alpha_{\text{p}} = 1$ and $\alpha_{\text{n}} = 1.067341$ are close to 1.

III. RESULTS

We first determine $r_{\text{n}}(\text{PREX2}) = 5.727 \pm 0.071$ fm and $r_{\text{m}}(\text{PREX2}) = 5.617 \pm 0.044$ fm from $r_{\text{p}}(\text{exp}) = 5.444$ fm [53] and $r_{\text{skin}}^{208}(\text{PREX2})$. The $r_{\text{p}}(\text{GHFB})$ calculated with D1S-GHFB+AMP agrees with $r_{\text{p}}(\text{exp}) = 5.444$ fm of electron scattering. For simplicity, we refer the D1S-GHFB+AMP proton density to as the PREX2 proton density in this paper. The neutron density calculated with GHFB+AMP is scaled so as to $r_{\text{n}}(\text{PREX2}) = 5.727$ fm. The resulting neutron density is referred to as the neutron PREX2 density in this paper.

Figure 3 shows E_{lab} of σ_{R} for ${}^3\text{He} + {}^{208}\text{Pb}$ scattering in $32 \leq E_{\text{lab}} \leq 56$ MeV per nucleon. The Kyushu g -matrix folding model with D1S-GHFB+AMP undershoots $\sigma_{\text{R}}(\text{exp})$ [10] in $32 \leq E_{\text{lab}} \leq 56$ MeV by a factor of 0.9344. This indicates that our results are good enough. The Kyushu g -matrix folding model with the PREX2 neutron and proton densities reproduces the data on σ_{R} at $E_{\text{lab}} = 32, 46, 56$ MeV per nucleon.

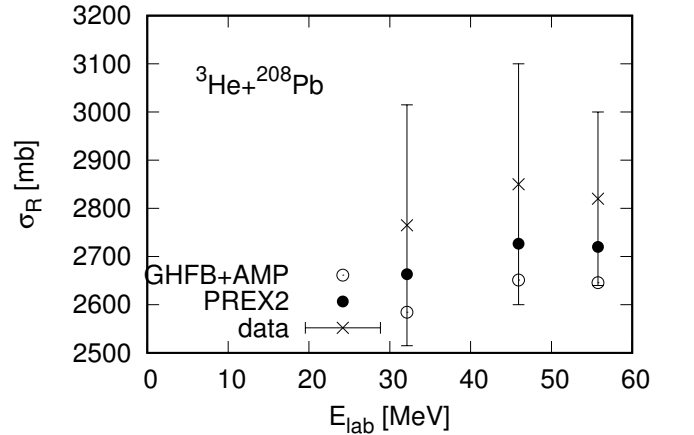


FIG. 3. E_{lab} dependence of reaction cross sections σ_{R} for ${}^3\text{He} + {}^{208}\text{Pb}$ scattering. Open circles stand for the results of the Kyushu G -matrix folding model with the D1S-GHFB+AMP densities. Closed circles correspond to the PREX2 proton and neutron densities. The data are taken from Refs. [10].

In $32 \leq E_{\text{lab}} \leq 56$ MeV per nucleon, we can obtain $r_{\text{m}}(\text{exp})$ from $\sigma_{\text{R}}(\text{exp})$ by scaling the D1S-GHFB+AMP densities so as to reproduce $\sigma_{\text{R}}(\text{exp})$ for each E_{lab} under the

condition that the proton radius of the scaling density agrees with the data $r_p(\text{exp}) = 5.444$ fm [53] of electron scattering, and take the weighted mean and its error for the resulting $r_m(\text{exp})$. From the resulting $r_m(\text{exp}) = 5.759 \pm 0.169$ fm and $r_p(\text{exp}) = 5.444$ fm of electron scattering, we can get $r_{\text{skin}}^{208}(\text{exp}) = 0.512 \pm 0.268$ fm and $r_n^{208}(\text{exp}) = 5.956 \pm 0.268$ fm.

The same procedure is taken for ${}^3,4\text{He}+{}^{58,60,64}\text{Ni}$ scattering. As for ${}^4\text{He}$, we take the data [10] in $30 \leq E_{\text{lab}} \leq 48$ MeV per nucleon for ${}^{58,60}\text{Ni}$ and the data [39] in $E_{\text{lab}} =$

8.8 MeV per nucleon for ${}^{64}\text{Ni}$. As for ${}^3\text{He}$, we take the data [10] in $32 \leq E_{\text{lab}} \leq 56$ MeV per nucleon for ${}^{58,60}\text{Ni}$ and the data [10] in $E_{\text{lab}} = 32$ MeV per nucleon for ${}^{64}\text{Ni}$. Our results are shown in Sec. I.

ACKNOWLEDGEMENTS

We thank Dr. Toyokawa for his contribution.

-
- [1] C. J. Horowitz, S. J. Pollock, P. A. Souder, and R. Michaels, *Phys. Rev. C* **63**, 025501 (2001).
- [2] S. Abrahamyan, Z. Ahmed, H. Albatineh, K. Aniol, D. S. Armstrong, W. Armstrong, T. Averett, B. Babineau, A. Barbieri, V. Bellini, et al. (PREX Collaboration), *Phys. Rev. Lett.* **108**, 112502 (2012).
- [3] C. J. Horowitz, Z. Ahmed, C.-M. Jen, A. Rakhman, P. A. Souder, M. M. Dalton, N. Liyanage, K. D. Paschke, K. Saenboonruang, R. Silwal, G. B. Franklin, M. Friend, B. Quinn, K. S. Kumar, D. McNulty, L. Mercado, S. Riordan, J. Wexler, R. W. Michaels, and G. M. Urciuoli, *Phys. Rev. C* **85**, 032501 (2012).
- [4] D. Adhikari et al. (PREX), *Phys. Rev. Lett.* **126**, 172502 (2021), arXiv:2102.10767 [nucl-ex].
- [5] X. Roca-Maza, M. Centelles, X. Vinas, and M. Warda, *Phys. Rev. Lett.* **106**, 252501 (2011), arXiv:1103.1762 [nucl-th].
- [6] R. F. Carlson, A. J. Cox, J. R. Nimmo, N. E. Davison, S. A. Elbahr, J. L. Horton, A. Houdayer, A. M. Sourkes, W. T. H. van Oers, and D. J. Margaziotis, *Phys. Rev. C* **12**, 1167 (1975).
- [7] A. Ingemarsson, J. Nyberg, P. Renberg, O. Sundberg, R. Carlson, A. Auce, R. Johansson, G. Tibell, B. Clark, L. Kurth Kerr, and S. Hama, *Nucl. Phys. A* **653**, 341 (1999).
- [8] A. Auce, A. Ingemarsson, R. Johansson, M. Lantz, G. Tibell, R. F. Carlson, M. J. Shachno, A. A. Cowley, G. C. Hillhouse, N. M. Jacobs, et al., *Phys. Rev. C* **71**, 064606 (2005).
- [9] S. Tagami, T. Wakasa, J. Matsui, M. Yahiro, and M. Takechi, *Phys. Rev. C* **104**, 024606 (2021), arXiv:2010.02450 [nucl-th].
- [10] A. Ingemarsson et al., *Nucl. Phys. A* **676**, 3 (2000).
- [11] M. Matsuzaki, S. Tagami, and M. Yahiro, *Phys. Rev. C* **104**, 054613 (2021), arXiv:2107.06441 [nucl-th].
- [12] J. C. Zamora et al., *Phys. Rev. C* **96**, 034617 (2017).
- [13] S. Tagami, T. Wakasa, M. Takechi, J. Matsui, and M. Yahiro, *Results in Physics* **33**, 105155 (2022).
- [14] A. Akmal, V. R. Pandharipande, and D. G. Ravenhall, *Phys. Rev. C* **58**, 1804 (1998), arXiv:nucl-th/9804027.
- [15] C. Ishizuka, T. Suda, H. Suzuki, A. Ohnishi, K. Sumiyoshi, and H. Toki, *Publ. Astron. Soc. Jap.* **67**, 13 (2015), arXiv:1408.6230 [nucl-th].
- [16] C. Gonzalez-Boquera, M. Centelles, X. Viñas, and L. M. Robledo, *Phys. Lett. B* **779**, 195 (2018), arXiv:1712.06735 [nucl-th].
- [17] M. Farine, D. Von-Eiff, P. Schuck, J. F. Berger, J. Dechargé, and M. Girod, **25**, 863 (1999).
- [18] C. Gonzalez-Boquera, M. Centelles, X. Viñas, and A. Rios, *Phys. Rev. C* **96**, 065806 (2017), arXiv:1706.02736 [nucl-th].
- [19] M. Oertel, M. Hempel, T. Klähn, and S. Typel, *Rev. Mod. Phys.* **89**, 015007 (2017), arXiv:1610.03361 [astro-ph.HE].
- [20] J. Piekarewicz, *Phys. Rev. C* **76**, 064310 (2007), arXiv:0709.2699 [nucl-th].
- [21] Y. Lim, K. Kwak, C. H. Hyun, and C.-H. Lee, *Phys. Rev. C* **89**, 055804 (2014), arXiv:1312.2640 [nucl-th].
- [22] R. Sellahewa and A. Rios, *Phys. Rev. C* **90**, 054327 (2014), arXiv:1407.8138 [nucl-th].
- [23] T. Inakura and H. Nakada, *Phys. Rev. C* **92**, 064302 (2015), arXiv:1509.02982 [nucl-th].
- [24] F. J. Fattoyev and J. Piekarewicz, *Phys. Rev. Lett.* **111**, 162501 (2013), arXiv:1306.6034 [nucl-th].
- [25] A. W. Steiner, M. Prakash, J. M. Lattimer, and P. J. Ellis, *Phys. Rept.* **411**, 325 (2005), arXiv:nucl-th/0410066.
- [26] M. Centelles, X. Roca-Maza, X. Vinas, and M. Warda, *Phys. Rev. C* **82**, 054314 (2010), arXiv:1010.5396 [nucl-th].
- [27] M. Dutra, O. Lourenco, J. S. Sa Martins, A. Delfino, J. R. Stone, and P. D. Stevenson, *Phys. Rev. C* **85**, 035201 (2012), arXiv:1202.3902 [nucl-th].
- [28] B. A. Brown and A. Schwenk, *Phys. Rev. C* **89**, 011307 (2014), [Erratum: *Phys.Rev.C* 91, 049902 (2015)], arXiv:1311.3957 [nucl-th].
- [29] B. A. Brown, *Phys. Rev. Lett.* **85**, 5296 (2000).
- [30] P. G. Reinhard, A. S. Umar, P. D. Stevenson, J. Piekarewicz, V. E. Oberacker, and J. A. Maruhn, *Phys. Rev. C* **93**, 044618 (2016), arXiv:1603.01319 [nucl-th].
- [31] C. Y. Tsang, B. A. Brown, F. J. Fattoyev, W. G. Lynch, and M. B. Tsang, *Phys. Rev. C* **100**, 062801 (2019), arXiv:1908.11842 [nucl-th].
- [32] C. Ducoin, J. Margueron, and C. Providencia, *EPL* **91**, 32001 (2010), arXiv:1004.5197 [nucl-th].
- [33] M. Fortin, C. Providencia, A. R. Raduta, F. Gulminelli, J. L. Zdunik, P. Haensel, and M. Bejger, *Phys. Rev. C* **94**, 035804 (2016), arXiv:1604.01944 [astro-ph.SR].
- [34] L.-W. Chen, C. M. Ko, B.-A. Li, and J. Xu, *Phys. Rev. C* **82**, 024321 (2010), arXiv:1004.4672 [nucl-th].
- [35] P. W. Zhao and S. Gandolfi, *Phys. Rev. C* **94**, 041302 (2016), arXiv:1604.01490 [nucl-th].
- [36] Z. Zhang, Y. Lim, J. W. Holt, and C. M. Ko, *Phys. Lett. B* **777**, 73 (2018), arXiv:1703.00866 [nucl-th].
- [37] Y. Wang, C. Guo, Q. Li, H. Zhang, Y. Leifels, and W. Trautmann, *Phys. Rev. C* **89**, 044603 (2014), arXiv:1403.7041 [nucl-th].
- [38] O. Lourenço, M. Bhuyan, C. H. Lenzi, M. Dutra, C. Gonzalez-Boquera, M. Centelles, and X. Viñas, *Phys. Lett. B* **803**, 135306 (2020), arXiv:2002.06242 [nucl-th].
- [39] L. V. L.V.Dubar, O.F.Nemets, “Total cross sections for reactions induced by alpha particles,” <http://www-nds.iaea.org/EXFOR/D5117.005> (1972).
- [40] M. Toyokawa, M. Yahiro, T. Matsumoto, and M. Kohno, *PTEP* **2018**, 023D03 (2018), arXiv:1712.07033 [nucl-th].
- [41] S. Tagami, M. Tanaka, M. Takechi, M. Fukuda, and M. Yahiro, *Phys. Rev. C* **101**, 014620 (2020), arXiv:1911.05417 [nucl-th].

- [42] M. Kohno, Phys. Rev. C **86**, 061301 (2012), arXiv:1209.5048 [nucl-th].
- [43] H. V. von Geramb et al., Phys. Rev. C **44**, 73 (1991).
- [44] K. Amos and P. J. Dortmans, Phys. Rev. C **49**, 1309 (1994).
- [45] F. A. Brieva and J. R. Rook, Nucl. Phys. **291**, 299 (1977).
- [46] F. A. Brieva and J. R. Rook, Nucl. Phys. **291**, 317 (1977).
- [47] F. A. Brieva and J. R. Rook, Nucl. Phys. **297**, 206 (1978).
- [48] K. Minomo, K. Ogata, M. Kohno, Y. R. Shimizu, and M. Yahiro, J. Phys. G **37**, 085011 (2010), arXiv:0911.1184 [nucl-th].
- [49] K. Egashira, K. Minomo, M. Toyokawa, T. Matsumoto, and M. Yahiro, Phys. Rev. C **89**, 064611 (2014).
- [50] T. Sumi, K. Minomo, S. Tagami, M. Kimura, T. Matsumoto, K. Ogata, Y. R. Shimizu, and M. Yahiro, Phys. Rev. C **85**, 064613 (2012), arXiv:1201.2497 [nucl-th].
- [51] H. de Vries, C. W. de Jager, and C. de Vries, At. Data Nucl. Data Tables **36**, 495 (1987).
- [52] B. Bonin et al., Nucl. Phys. A **445**, 381 (1985).
- [53] B. A. Brown, Phys. Rev. Lett. **111**, 232502 (2013), arXiv:1308.3664 [nucl-th].